



OPEN

Single domain intrabodies against WASP inhibit TCR-induced immune responses in transgenic mice T cells

SUBJECT AREAS:

IMMUNOLOGICAL
TECHNIQUES

MOLECULAR BIOLOGY

SIGNAL TRANSDUCTION

T-CELL RECEPTOR

Mitsuru Sato, Ryoko Sawahata, Chisato Sakuma, Takato Takenouchi & Hiroshi Kitani

Animal Immune and Cell Biology Research Unit, National Institute of Agrobiological Sciences, 1-2 Ohwashi, Tsukuba, Ibaraki 305-8634, Japan.

Received
21 May 2013Accepted
4 October 2013Published
21 October 2013Correspondence and
requests for materials
should be addressed to
H.K. (kitani@affrc.go.
ip)

Intrabody technology provides a novel approach to decipher the molecular mechanisms of protein function in cells. Single domains composed of only the variable regions (V_H or V_L) of antibodies are the smallest recombinant antibody fragments to be constructed thus far. In this study, we developed transgenic (Tg) mice expressing the V_H or V_L single domains derived from a monoclonal antibody raised against the N-terminal domain of Wiskott–Aldrich syndrome protein (WASP), which is an adaptor molecule in immune cells. In T cells from anti-WASP V_H and V_L single domain Tg mice, interleukin-2 production induced by T cell receptor (TCR) stimulation were impaired, and specific interaction between the WASP N-terminal domain and the Fyn SH3 domain was strongly inhibited by masking the binding sites in WASP. These results strongly suggest that the V_H/V_L single domain intrabodies are sufficient to knockdown the domain function of target proteins in the cytosol.

Intracellularly expressed antibody fragments (intrabodies) have been used as powerful tools for clinical applications and for basic studies of intracellular protein function. Specific binding of intrabodies to the target domain selectively inhibits the function of intracellular proteins. A standard intrabody structure is a single chain variable fragment (scFv), which is composed of one heavy chain variable region (V_H) linked through a flexible peptide spacer (GGGGS \times 3) to one light chain variable region (V_L). The scFv intrabodies retain specificity and affinity similar to the parental antibody^{1,2}, and have been applied successfully in basic research to achieve the functional knockdown of intracellular targets, such as human immunodeficiency virus (HIV) gp120³, chemokine receptor⁴, growth factor receptor⁵, oncogenic Ras protein⁶, and p53 tumor suppressor⁷. However, the expression and function of scFv in the cytoplasm is often hampered by the misfolding, degradation, or aggregation of scFv due to reduced conditions in the cytoplasm⁸. In some cases, owing to the lack of disulfide bonds, scFv molecules fail to adopt the proper conformation associated with antigen binding⁹.

Several possible modifications of intrabodies may enhance their stability and functional activity in the cytoplasmic environment, thereby overcoming these problems. For example, in nature, camelids have evolved homodimeric heavy-chain antibodies, which completely lack the light-chain, as part of their humoral immune response¹⁰. This phenomenon suggests that a single variable domain fragment of antibody, either V_H or V_L alone, may be sufficient to function as an intrabody¹¹.

Wiskott–Aldrich syndrome (WAS) protein (WASP), the gene product responsible for X-linked immunodeficiency^{12,13}, is predominantly expressed in the cytosol of hematopoietic cells and regulates immune responses, such as the production of interleukin (IL)-2 and the reorganization of actin filaments in T cell receptor (TCR) signaling. T cells from WASP-deficient mice exhibit a marked reduction in antigen receptor capping and actin polymerization induced by TCR stimulation^{14,15}. In addition to these cytoskeletal abnormalities, TCR stimulation induces impaired IL-2 production in T cells from WAS patients and WASP-deficient mice^{14–16}.

Most of the gene mutations in WAS patients have been mapped to the WASP N-terminal region, including the Enabled/vasodilator-stimulated protein (Ena/VASP) homology 1 (EVH1) domain, suggesting that this domain is indispensable for WASP function¹⁷. To investigate further the function of the WASP N-terminal domain in the TCR signaling pathway, we previously developed transgenic (Tg) mice that overexpress WASP N-terminal exons 1–5 (aa1–171, designated WASP15). T cells from WASP15 Tg mice were impaired in their proliferation and IL-2 production induced by TCR stimulation, owing to the dominant negative effects of the overexpressed WASP15. In contrast, antigen receptor capping and actin polymerization were unaffected¹⁸. The functions of the WASP N-terminal domain were confirmed in Tg mice expressing scFv intrabodies that specifically bound this domain. The



expression of anti-WASP scFv intrabodies inhibited TCR-stimulation-induced IL-2 production without affecting TCR capping in T cells from anti-WASP scFv Tg mice¹⁹. These results strongly suggested that the WASP N-terminal domain plays a pivotal role in IL-2 production, but not in antigen receptor capping in the TCR signaling pathway.

To extend our earlier work in intrabody technologies, we previously constructed four types of single domain intrabodies derived from the anti-WASP N-terminus monoclonal antibody. These single domains were composed of the V_H and V_L regions with or without their leader sequences. These single domains were expressed at similar levels and showed the specific binding activity to the WASP N-terminal domain in gene-transfected NIH3T3 cells²⁰. In this study, to assess the ability to inhibit IL-2 production upon TCR stimulation through the expression of anti-WASP single domain intrabodies in T cells, we developed Tg mice that expressed anti-WASP single domains. Anti-WASP single domains efficiently bound to WASP in these Tg mouse T cells, and their inhibitory effects on IL-2 production upon TCR stimulation were similar to those of anti-WASP scFv.

Results

Expression of anti-WASP scFv and single domains in gene-transfected T cells. Previously, we constructed two types of scFv¹⁹ and four types of single domains²⁰ derived from the anti-WASP N-terminus monoclonal antibody with or without the leader sequences of the V_H and V_L region (Fig. 1a). To compare the expression levels of these scFv and single domains, the DNA constructs were transiently transfected into DO11-10 murine T cell hybridomas. In gene-transfected murine T cells high expression of the scFv and single domain constructs with leader sequences, SHL, SV_H, and SV_L, was observed, whereas the constructs without leader sequences, HL and V_H, were showed lower expression levels and expression of V_L was hardly detected in the western blot analysis with anti-Myc tag antibody (Fig. 1b, upper panel). Quite similar to DO11-10 murine T cells, expression levels of SHL, SV_H, and SV_L were higher than those of HL, V_H, and V_L in gene-transfected human Jurkat T cells (Fig. 1c, upper panel), suggesting that the expression efficiency of scFv and single domain constructs is dependent on the presence of leader sequences in T lymphocytes. The amounts of protein loaded in each lane were confirmed by Western blotting with anti-β-actin antibody (Fig. 1b and 1c, lower panel). We previously demonstrated that all of the single domains, SV_H, V_H, SV_L, and V_L were expressed at comparable levels in gene-transfected NIH3T3 cells²⁰. So, the expression efficiency of scFvs and single domains is variable between T lymphocytes and NIH3T3 fibroblasts, highly dependent on the presence of leader sequences in the former cell type.

Expression of SV_H/SV_L single domain and specific binding to WASP in T cells from Tg mice. As SV_H and SV_L DNA constructs containing their leader sequences were strongly expressed in gene-transfected T cells, we used these constructs for the development of transgenic mice to knockdown WASP N-terminal domain function (Fig. 1a). Tg mice expressing the WASP N-terminal domain (WASP15) and anti-WASP scFv with the leader signal sequence of the V_H region (SHL) had been established previously (Fig. 1a)^{18,19}.

Two independent SV_H (a and b) Tg and three independent SV_L (c, d, and e) Tg founders were established, and T cells from C57BL/6, anti-WASP SHL Tg, SV_H (a and b) Tg, and SV_L (c, d, and e) Tg mice were lysed and immunoprecipitated with anti-Myc tag antibody. The expression pattern of anti-WASP SHL and SV_L was similar to that of their transient expression in DO11-10 or Jurkat T cells (Fig. 1d, lower panel). Whereas SV_H were expressed at the size of 18 kDa, and the additional two bands were detected as upper size of 20 kDa and 23 kDa. These bands may indicate the products from the transgenes of SV_H DNA construct or some unrelated proteins, which are

cross-reacted with anti-Myc-tag antibody (Fig. 1d, lower panel). In this immunoprecipitation analysis, all single domains exhibited their efficient binding activity to WASP (Fig. 1d, upper panel). As a result, SV_H-b and SV_L-d Tg lines were used for the following experiments.

N-WASP, a ubiquitously expressed homologue of WASP, shares 50% sequence similarity with WASP and it contains the EVH1 domain²¹. However, the binding of N-WASP and anti-WASP SHL, SV_H, and SV_L intrabodies was not observed in these Tg mice T cells (Fig. S1), suggesting that these anti-WASP intrabodies specifically binds to the WASP N-terminal domain in Tg mice T cells.

Subcellular localization of anti-WASP SV_H/SV_L single domains in T cells from Tg mice. To examine the subcellular localization of anti-WASP SV_H/SV_L single domains, T cells from anti-WASP SHL-Tg, SV_H-Tg, and SV_L-Tg mice were fractionated into their subcellular compartments, and each fractions were analyzed by Western blotting with anti-Myc tag antibody. In Tg T cells, anti-WASP SHL, SV_H, and SV_L were detected in both the cytosolic and membrane fractions, although the levels were higher in the latter fraction (Fig. 1e, upper panel). In general, antibodies with the leader signal sequences cross the rough endoplasmic reticulum (ER) membrane and enter the secretory pathway through the *trans*-Golgi network. However, some of anti-WASP scFv and single domains with leader sequences were detected in the cytoplasm. Although the reason and mechanism remained unknown, these scFv and single domains reside in the cytoplasm and efficiently bind to the target proteins as intrabodies. To validate each subcellular fraction, WASP (Fig. 1e, center panel) and Ribophorin I (Fig. 1e, lower panel) were detected by specific antibodies as cytosolic and membrane protein markers, respectively. These results demonstrated that neither fraction was cross-contaminated by the other fraction.

T cell development in WASP15-Tg, anti-WASP SHL-Tg, SV_H-Tg, and SV_L-Tg mice was similar to wild-type mice (Fig. S2), suggesting that overexpressed WASP15, anti-WASP SHL, SV_H, and SV_L do not have any adverse effect on lymphocyte development.

Impairment of IL-2 production in anti-WASP SV_H/SV_L single domain Tg T cells upon TCR stimulation. To assess the effects of anti-WASP SV_H/SV_L single-domain expression on IL-2 transcription, quantitative real-time PCR was performed using RNA isolated from the T cells of wild-type, WASP15-Tg, anti-WASP SHL-Tg, SV_H-Tg, and SV_L-Tg mice after TCR stimulation. In contrast to the apparent upregulation of IL-2 gene transcription upon TCR stimulation in wild-type T cells, T cells from WASP15-Tg mice exhibited less than one-third and T cells from anti-WASP SHL-Tg, SV_H-Tg, and SV_L-Tg mice exhibited approximately one-half of the levels of IL-2 transcription (Fig. 2a). The basal gene transcription of IL-2 was undetectable level in all mice T cells (data not shown). Impairment of IL-2 secretion from these Tg T cells was confirmed by ELISA (Fig. 2b), indicating that the function of the WASP N-terminal region (including the EVH1 domain) for IL-2 production upon TCR stimulation is inhibited by SV_H/SV_L single domain intrabodies in T cells from Tg mice. T cells from another SV_H transgenic line and two additional SV_L transgenic lines exhibited similarly impaired IL-2 production upon TCR stimulation (data not shown), suggesting that copy number and integration site had no adverse effects on the transgene.

Impaired antigen receptor-induced proliferation in anti-WASP SV_H/SV_L single domain Tg T cells. To assess the effects of anti-WASP SV_H/SV_L single domain expression on T cell function, the proliferative response to stimulation with anti-CD3ε antibody was examined. In parallel to IL-2 production upon TCR stimulation, T cells from each Tg mouse line exhibited reduced proliferative responses compared with wild-type T cells: respectively, WASP15-Tg, anti-WASP SHL Tg, SV_H Tg, and SV_L Tg T cells exhibited one-third, two-thirds, one-half, and one-half of the proliferative response

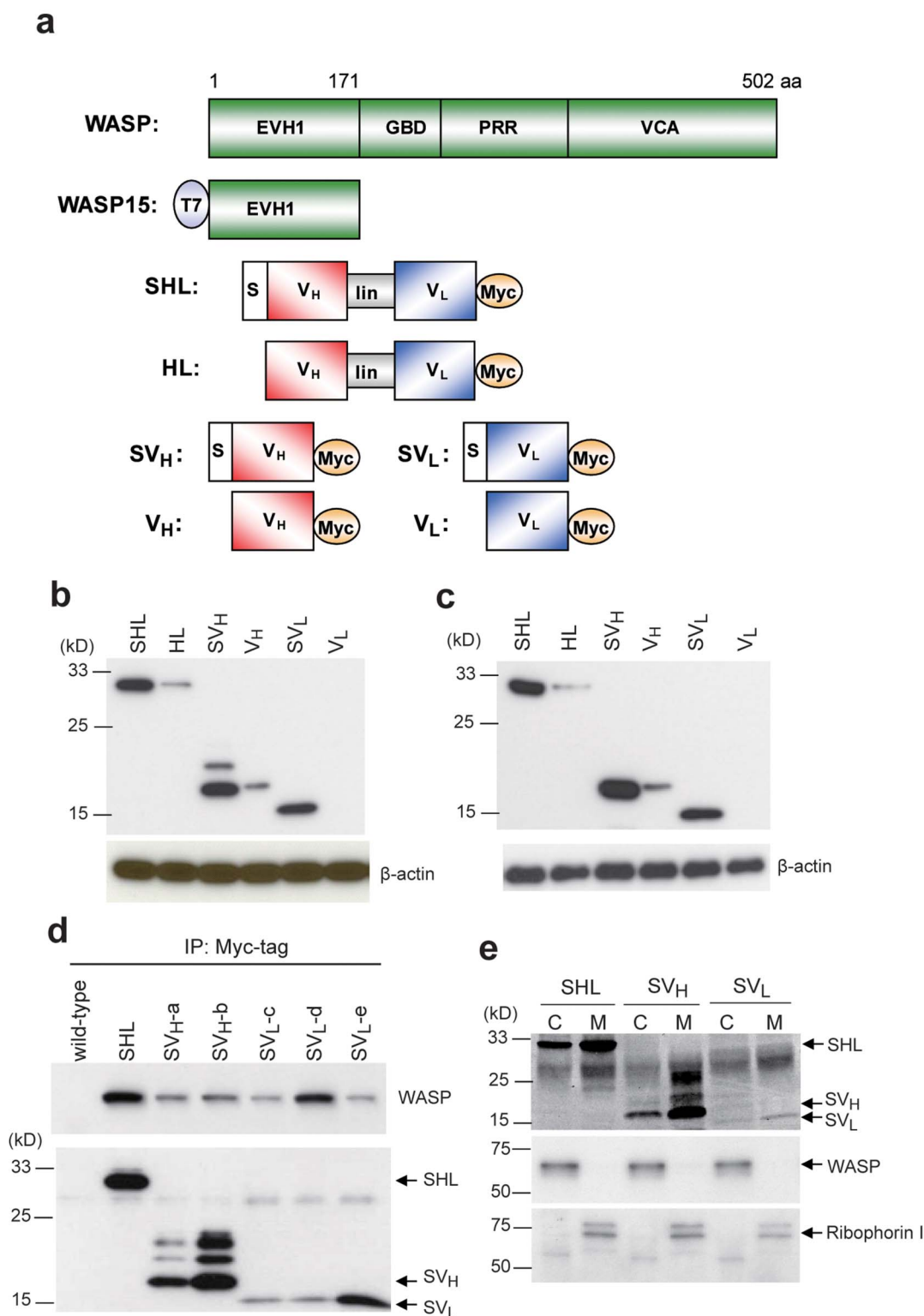


Figure 1 | Expression and binding activity of anti-WASP SHL, SV_H, and SV_L intrabodies in T cells from Tg mice. (a) Schematic representation of WASP, truncated WASP (WASP15), anti-WASP SHL, HL, SV_H, V_H, SV_L, and V_L constructs. The major functional domains of WASP [the EVH1 domain (EVH1), GTPase-binding domain (GBD), proline rich region (PRR), and verproline/cofilin/acidic domain (VCA)], the leader signal sequence (S), the V_H and V_L regions of anti-WASP N-terminus mAb, the flexible peptide liker (lin), and the T7- and Myc-tagged sequences are shown. (b) DO11-10 T cells and (c) Jurkat T cells were transfected with DNA encoding anti-WASP scFv and single domain derivatives. Western blot analysis showing the expression levels of each scFvs and single domains in transfected T cells. The immunoblots were probed with anti-Myc-tag pAb or anti-β-actin pAb. (d) T cells from wild-type, anti-WASP SHL Tg, SV_H (a and b) Tg, and SV_L (c, d, and e) Tg mice were lysed and immunoprecipitated (IP) with anti-Myc-tag mAb. Immunocomplexes were analyzed by Western blotting with anti-WASP pAb or anti-Myc-tag pAb. (e) T cell extracts from anti-WASP SHL, SV_H, and SV_L Tg mice were separated into cytosolic (C) and membrane (M) fractions. The fractionated cell extracts were analyzed by Western blotting with anti-Myc-tag pAb, anti-WASP pAb, or anti-Ribophorin I pAb. Full-length gels/blots are presented in Supplemental Fig. 1. Immunoblots are representative of three independent experiments.

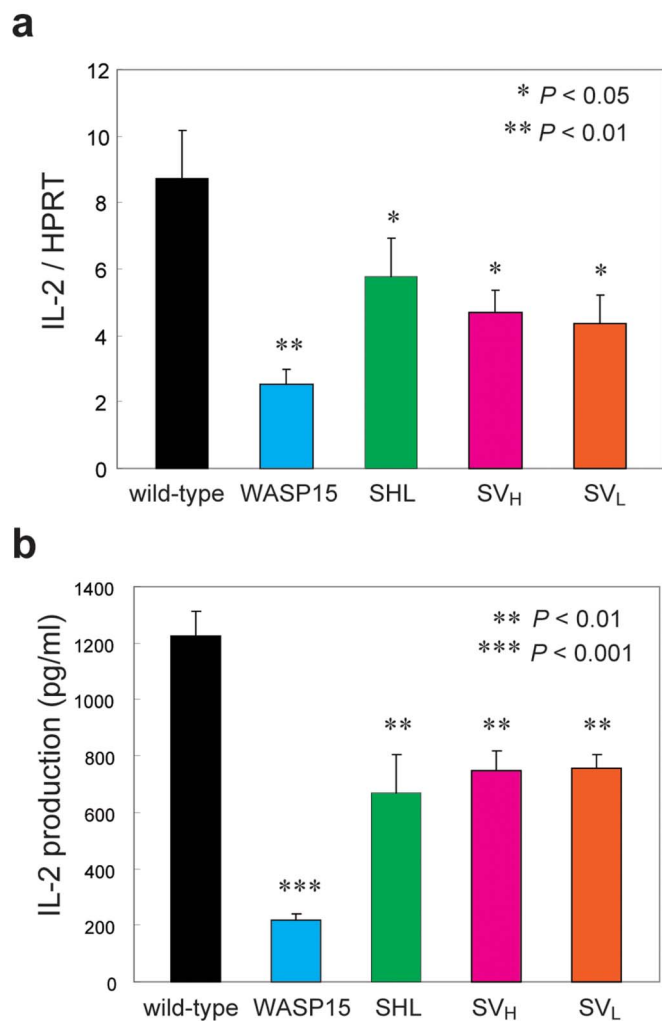


Figure 2 | Impaired IL-2 production after TCR stimulation in WASP15 Tg, anti-WASP SHL Tg, SV_H Tg, and SV_L Tg T cells. (a) Quantitative real-time PCR was performed on RNA derived from T cells from wild-type, WASP15 Tg, anti-WASP SHL Tg, SV_H Tg, and SV_L Tg mice after TCR stimulation. Expression levels are reported as IL-2 transcript per control HPRT transcript. (b) Purified T cells from the spleens of wild-type, WASP15 Tg, anti-WASP SHL Tg, SV_H Tg, and SV_L Tg mice were cultured in anti-CD3 ϵ antibody-coated dishes (see Experimental procedures). IL-2 protein in the supernatant was quantified by ELISA. Values are expressed as mean \pm SEM from three independent experiments. Statistical significance is indicated by * $P < 0.05$, ** $P < 0.01$, and *** $P < 0.001$.

exhibited by wild-type T cells (Fig. 3a). The addition of exogenous IL-2 restored the normal proliferative response to anti-CD3 ϵ antibody stimulation in all Tg T cells (Fig. 3b). The basal cell proliferation was undetectable level in all mice T cells (data not shown). These findings indicate that the WASP N-terminal domain has a critical role in signaling through the TCR, but not the IL-2 receptor.

In contrast to the impairment of IL-2 production and antigen receptor-induced proliferation, T cells from each Tg mouse line exhibited normal actin polymerization induced by TCR stimulation (Fig. S3). Furthermore, immunofluorescent microscopy demonstrated that the extent of antigen receptor capping induced by TCR stimulation in all Tg mice T cells was similar to that in the wild-type mice (Fig. S4). These results strongly suggest that anti-WASP SHL, SV_H, and SV_L intrabodies specifically inhibit the WASP N-terminal domain function for IL-2 production, but do not affect the actin cytoskeletal rearrangement induced by TCR stimulation.

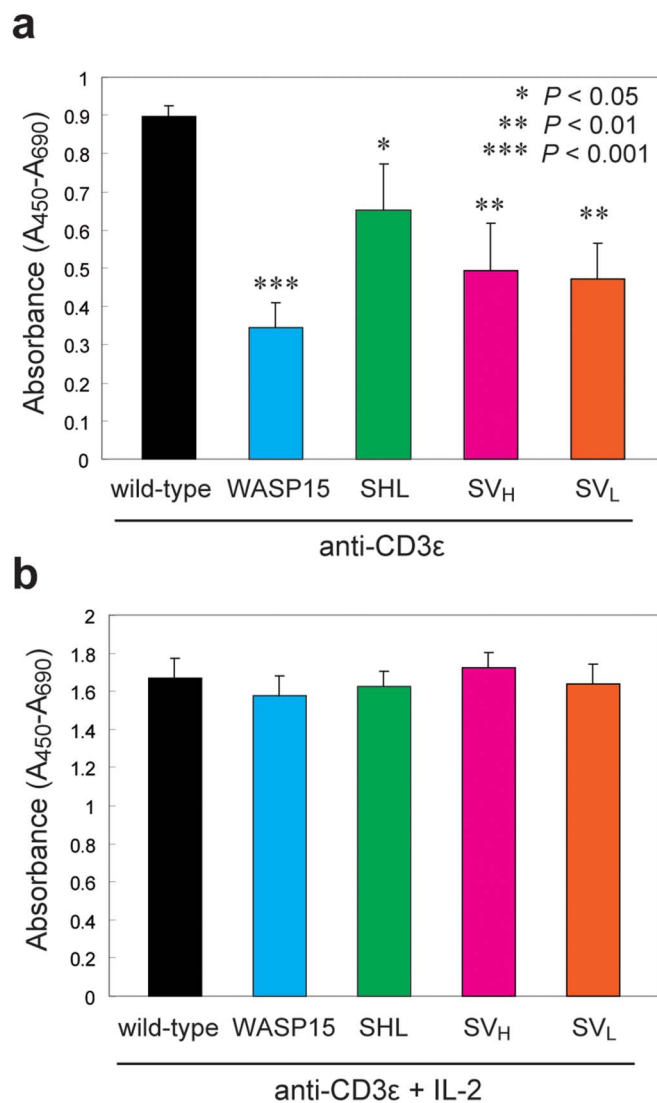


Figure 3 | TCR-induced proliferation in wild-type, WASP15 Tg, anti-WASP SHL Tg, SV_H Tg, and SV_L Tg mice. Purified T cells from the spleens of wild-type, WASP15 Tg, anti-WASP SHL Tg, SV_H Tg, and SV_L Tg mice were cultured in anti-CD3 ϵ antibody-coated plates (see Experimental procedures). Each stimulation was performed in the absence (a) or presence (b) of exogenous IL-2 as indicated. After incubation for 48 h, 10 μ M BrdU was added to the T cell cultures. The cells were incubated for an additional 16 h, and BrdU incorporation was quantified by ELISA. Values are expressed as mean \pm SEM from triplicate cultures, and are representative of three independent experiments. Statistical significance is indicated by * $P < 0.05$, ** $P < 0.01$, and *** $P < 0.001$.

Lymphoid cells from anti-WASP SV_H/SV_L Tg mice immunized with ovalbumin exhibited impaired proliferative response and IL-2 production induced by secondary ovalbumin stimulation.

To assess the effect of anti-WASP SV_H/SV_L single domain expression on lymphoid cells, a proliferation assay was performed on lymphoid cells derived from wild-type, WASP15-Tg, anti-WASP SHL-Tg, SV_H-Tg, and SV_L-Tg mice immunized with ovalbumin (OVA). Single cell suspensions from the lymph nodes of OVA-immunized wild-type and all Tg mice were cultured with OVA or control bovine serum albumin (BSA) for 48 h. In contrast to the upregulating proliferation observed upon secondary OVA stimulation in wild-type lymphoid cells, lymphoid cells from all Tg mice exhibited an impaired proliferative response to secondary OVA stimulation (Fig. 4a). In particular, the inhibitory effects of SV_L in the



proliferative response to secondary OVA stimulation were similar to those of WASP15 and anti-WASP SHL (Fig. 4a). As a negative control, lymphoid cells derived from OVA-immunized wild-type and all Tg mice did not proliferate in response to nonspecific antigen stimulation with BSA (Fig. 4a).

To evaluate IL-2 production induced by the specific antigen, single cell suspensions from lymph nodes of wild-type, WASP15 Tg, anti-WASP SHL Tg, SV_H Tg, and SV_L Tg mice immunized with OVA were cultured with OVA for 24 h. In contrast to marked upregulation of IL-2 production in response to secondary OVA stimulation in wild-type lymphoid cells, lymphoid cells from WASP15 Tg and anti-WASP SHL Tg mice exhibited only one-fifth and lymphoid cells from anti-WASP SV_H/SV_L single domain Tg mice exhibited one-half of wild-type IL-2 production levels (Fig. 4b). These findings indicate that expression of anti-WASP SV_H/SV_L single domains induces impairment of the T cell immune response to the specific antigen in Tg mice.

Inhibition of the specific interaction between Fyn and WASP by expressing anti-WASP SV_H/SV_L single domain intrabodies. Recently, we demonstrated that the SH3 domain of Fyn is a binding partner of the WASP N-terminal domain in mouse T cells, and that the inhibition of this interaction by the overexpression of WASP15 and anti-WASP scFv resulted in impaired IL-2 synthesis upon TCR stimulation²². To assess the inhibitory effect of anti-WASP SV_H/SV_L single domain expression on the specific interaction between Fyn and WASP, T cell lysates from wild-type, WASP 15 Tg, anti-WASP SHL Tg, SV_H Tg, and SV_L Tg mice were incubated with glutathione S-transferase (GST) or GST-Fyn-SH3 fusion proteins, and pulled down with glutathione sepharose beads. In contrast to the strong binding of WASP to the GST-Fyn-SH3 in wild-type T cells, their interactions were markedly inhibited in T cells from WASP 15 Tg, anti-WASP SHL Tg, SV_H Tg, and SV_L Tg mice (Fig. 5a, upper panel). The protein levels of GST and GST-Fyn-SH3 were comparable in the assay (Fig. 5a, lower panel). The expression levels of WASP in T cells from wild-type and each Tg mice were confirmed by Western blotting with anti-WASP and anti-β-actin antibodies (Fig. 5b).

To confirm the inhibitory effect of the anti-WASP SV_H/SV_L single domain on the specific binding between endogenous Fyn and WASP in T cells, T cell lysates from wild-type, WASP15 Tg, anti-WASP SHL Tg, SV_H Tg, and SV_L Tg mice were immunoprecipitated with a monoclonal antibody (mAb) raised against Fyn, and immunocomplexes were immunoblotted with anti-WASP antibody. In the immunoprecipitation analysis, specific binding between endogenous Fyn and WASP was clearly detected in wild-type T cells (Fig. 5c, upper panel). In contrast, the interaction between Fyn and WASP was severely inhibited in WASP15 Tg T cells (Fig. 5c, upper panel). In addition, competitive binding of the truncated WASP to Fyn was demonstrated by immunoblotting with anti-T7-tag antibody (Fig. 5c, center panel). The production of anti-WASP SHL, SV_H, or SV_L intrabodies also inhibited the binding of Fyn and WASP (Fig. 5c, upper panel). Fyn was equivalently immunoprecipitated in T cells from all mouse lines (Fig. 5c, lower panel). These observations demonstrate that anti-WASP SV_H/SV_L single domains inhibit the Fyn-WASP interaction by masking the WASP N-terminal domain, and their abilities are comparable to scFv intrabody in T cells from Tg mice.

Inhibition of the interaction between WASP N-terminal domain and WIP by expressing anti-WASP SV_H/SV_L single domain intrabodies. WASP-interacting protein (WIP) is known to bind to the WASP N-terminal EVH1 domain²³. Previously, we demonstrated that the overexpression of WASP15 or anti-WASP scFv inhibits the interaction between WASP N-terminal domain and WIP in each Tg mice T cells²². To assess the inhibitory effect of anti-WASP SV_H/SV_L single domain expression on WIP-WASP interaction, T cell lysates from wild-type, WASP15 Tg, anti-WASP SHL Tg, SV_H Tg, and SV_L Tg mice were immunoprecipitated with anti-WIP antibody, and immunocomplexes were immunoblotted with anti-WASP antibody. In wild-type T cells, a strong binding between WIP and WASP was observed (Fig. 5d, upper panel). In contrast, the WIP-WASP interaction was greatly inhibited in WASP15 Tg and anti-WASP SHL Tg T cells, and anti-WASP SV_H/SV_L expression was also effectively inhibited the WIP-WASP

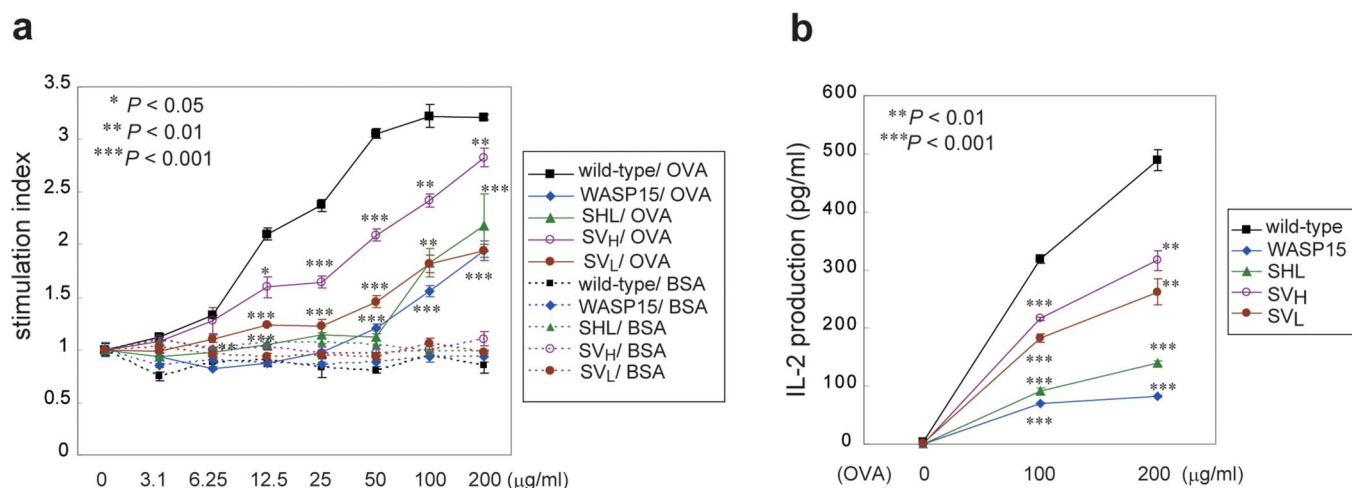


Figure 4 | Proliferative response and IL-2 production of lymphoid cells from wild-type, WASP15 Tg, anti-WASP SHL Tg, SV_H Tg, and SV_L Tg mice stimulated with OVA. Mice were immunized in both footpads with 100 µg of OVA in TiterMax gold (water-in oil adjuvant) (day 0). Inguinal, popliteal, and periaortic lymph nodes were removed, and single cell suspensions were prepared in RPMI 1640 medium (day 7). (a) Cells (1×10^5) were seeded in each well of 96-well tissue culture plates and cultured with the indicated amount of OVA or control BSA at 37°C for 48 h, then 10 µM BrdU was added to the lymphoid cell cultures. The cells were incubated for an additional 16 h, and then BrdU incorporation was quantified by ELISA. Stimulation indices (see Experimental procedures) were calculated using the arithmetic mean values of triplicate cultures. (b) Lymphoid cells (1×10^6) were cultured with the indicated amount of OVA in 48-well tissue culture plates for 24 h. The IL-2 levels in culture supernatants were quantified by ELISA. Values are expressed as mean \pm SEM from triplicate cultures, and are representative of three independent experiments. Statistical significance is indicated by * $P < 0.05$, ** $P < 0.01$, and *** $P < 0.001$.

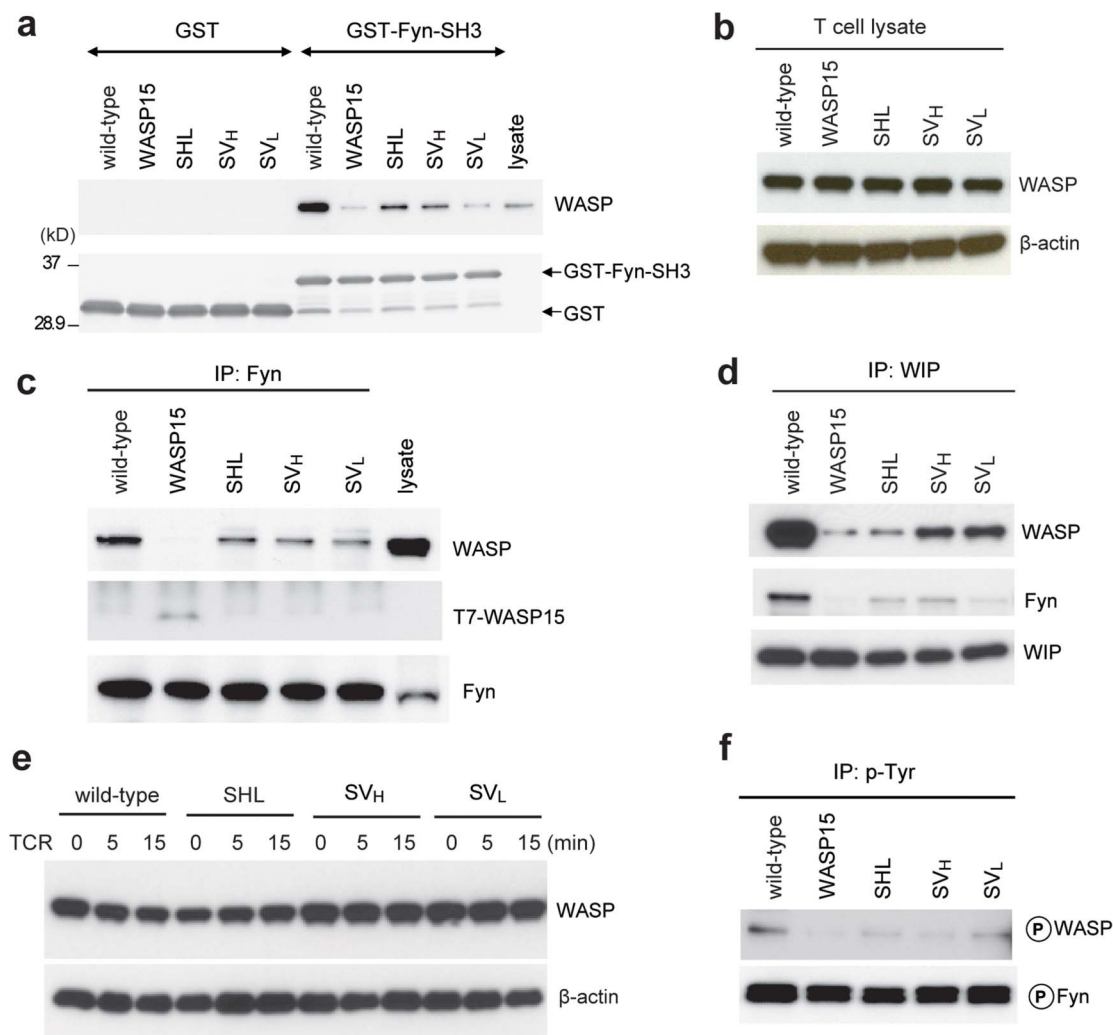


Figure 5 | Inhibition of the WASP-Fyn and WASP-WIP interactions by anti-WASP SHL, SV_H, and SV_L intrabodies. (a) T cells from the spleens of wild-type, WASP15 Tg, anti-WASP SHL Tg, SV_H Tg, and SV_L Tg mice were lysed and incubated with GST or GST-Fyn-SH3 fusion protein non-covalently bound to glutathione sepharose beads. Bound proteins were analyzed by Western blotting with anti-WASP pAb or anti-GST pAb. (b) The protein levels of WASP and β -actin in each Tg T cells were examined by immunoblotting. (c) T cell lysates of wild-type, WASP15 Tg, anti-WASP SHL Tg, SV_H Tg, and SV_L Tg mice were immunoprecipitated (IP) with anti-Fyn mAb. Immunocomplexes were analyzed by Western blotting with anti-WASP pAb, anti-T7 pAb, or anti-Fyn pAb. (d) T cell lysates of wild-type, WASP15 Tg, anti-WASP SHL Tg, SV_H Tg, and SV_L Tg mice were immunoprecipitated (IP) with anti-WIP antibody. Immunocomplexes were analyzed by Western blotting with anti-WASP pAb, anti-Fyn pAb or anti-WIP pAb. (e) T cells from wild-type, anti-WASP SHL, SV_H, and SV_L Tg mice were stimulated with anti-CD3 ϵ antibody for the period indicated, lysed, and analyzed by Western blotting with anti-WASP pAb or anti- β -actin pAb. (f) Purified T cells from the spleens of wild-type, WASP15 Tg, anti-WASP SHL Tg, SV_H Tg, and SV_L Tg mice with TCR stimulation were lysed and immunoprecipitated (IP) with anti-phosphotyrosine (p-Tyr) mAb. Immunocomplexes were analyzed by Western blotting with anti-WASP pAb or anti-Fyn pAb. Full-length gels/blots are presented in Supplemental Fig. 5. Immunoblots are representative of three independent experiments.

interaction (Fig. 5d, upper panel). These results suggest that the WASP N-terminal domain has an affinity to WIP in T cells.

Furthermore, to demonstrate the Fyn-WIP complex in TCR signaling, immunoprecipitates with anti-WIP antibody were immunoblotted with anti-Fyn pAb. The interaction of Fyn was clearly detected in wild-type T cells. However, by expression of WASP15, anti-WASP SHL, SV_H, and SV_L the binding of Fyn was inhibited in each Tg mice T cells (Fig. 5d, center panel). WIP was equivalently immunoprecipitated in all mice T cells (Fig. 5d, lower panel). These results strongly suggest that Fyn, WASP, and WIP are closely associated in the complex to modulate TCR-induced immune response.

In T cells from WIP knockout mice, the expression of WASP was severely diminished, suggesting that the binding of WIP and WASP is necessary for the stabilization of WASP²⁴. To assess whether the expression of anti-WASP SHL, SV_H, and SV_L intrabodies affects the stability of WASP in T cells, expression levels of

WASP were compared among wild-type, anti-WASP SHL, SV_H, and SV_L Tg T cells. The expression levels of WASP were similar in all mice T cells regardless of the TCR stimulation (Fig. 5e, upper panel). The amounts of protein loaded in each lane were confirmed by Western blotting against β -actin (Fig. 5e, lower panel). These results suggest that expression of anti-WASP-SHL, SV_H, and SV_L intrabodies, which strongly inhibits the binding of WIP and WASP, does not affect the expression and stability of WASP in T cells. So far, we do not know exactly how WASP is stabilized without the interaction with WIP in these anti-WASP SHL, SV_H, SV_L Tg mice. It may be possible that binding of anti-WASP intrabodies to EVH1 domain stabilize WASP, but this speculation needs to be verified.

Impaired tyrosine phosphorylation of WASP in anti-WASP SV_H/SV_L single domain Tg T cells upon TCR stimulation. We previously



demonstrated that overexpression of the WASP N-terminal domain and anti-WASP scFv affects TCR-stimulation-induced tyrosine phosphorylation of WASP²². To assess whether the expression of anti-WASP SV_H/SV_L single domains affects TCR-stimulation-induced tyrosine phosphorylation, the extent of TCR-induced tyrosine phosphorylation of WASP was compared among wild-type, WASP15 Tg, anti-WASP SHL Tg, SV_H Tg, and SV_L Tg T cells by immunoprecipitation analysis. Tyrosine phosphorylation of WASP upon TCR stimulation was clearly detected in wild-type T cells, but was effectively reduced in anti-WASP SV_H/SV_L Tg T cells (Fig. 5f, upper panel). In contrast, Fyn was equivalently tyrosine phosphorylated upon TCR stimulation among all T cells from all mouse lines (Fig. 5f, lower panel). These results suggest that overexpression of the WASP N-terminal domain, anti-WASP N-terminus SHL, SV_H, or SV_L inhibits tyrosine phosphorylation of WASP by interrupting the binding of Fyn-SH3 to the WASP N-terminus, but does not affect the activation of Fyn upon TCR stimulation.

NFAT pathway activation induced by TCR stimulation in WASP15 Tg, anti-WASP SHL Tg, SV_H Tg, and SV_L Tg T cells. Upon TCR stimulation, activated NFAT translocates from the cytosol into the nucleus, and induces IL-2 transcription^{25,26}. In our recent study, nuclear translocation of NFATc2, a member of the NFAT family, was deficient in WASP15 Tg T cells after TCR stimulation²². To assess the effects of anti-WASP SHL or SV_H/SV_L single domain expression on the nuclear translocation of NFATc2, T cells from wild-type, WASP15 Tg, anti-WASP SHL Tg, SV_H Tg, and SV_L Tg mice were fractionated into their subcellular components, and each fraction was analyzed by Western blotting with anti-NFATc2 antibody. NFATc2 was detected similarly in the cytosolic fraction of T cells from all mouse lines and protein levels of each cytosolic fraction were confirmed by Western blotting against β -actin (Fig. 6a). In wild-type T cells, nuclear translocation of NFATc2 was detected after 5 min of TCR stimulation, and increased at 15–30 min after TCR stimulation. However, in WASP15 Tg, anti-WASP SHL Tg, SV_H Tg, and SV_L Tg T cells, the nuclear translocation of NFATc2 was strongly inhibited in this assay (Fig. 6b). Blotting was performed with anti-HDAC1 antibody used as a nuclear fraction marker to validate the subcellular fractionation and the amount of protein loaded in each lane (Fig. 6b). These results suggest that masking of the WASP N-terminal domain by anti-WASP SHL or SV_H/SV_L intrabody effectively inhibits NFATc2 activation after TCR stimulation. Taken together, these results strongly imply that the WASP N-terminal domain is important for WASP function in IL-2 production mediated by the nuclear translocation of NFATc2 in stimulated T cells.

Discussion

In the present study we demonstrated that intracellularly expressed SV_H and SV_L single domain intrabodies, the simplest intrabody structure derived from the variable region of the original mAb, retain their specific binding activity to the target signaling molecule and efficiently inhibit the TCR-induced immune response in a Tg mouse model.

Single domain intrabodies have several benefits in comparison to standard intrabodies to study the molecular mechanisms of protein function in the cells. Single domain intrabodies are the simplest in structure, composed of either V_H or V_L alone, but still work as intrabody without intradomain disulfide bonds in murine NIH3T3 cells²⁰, and T cells from Tg mice, as demonstrated in the present study. As Tanaka et al²⁷, suggested regarding anti-Ras V_H/V_L fragments, intradomain disulfide bonds may not be required for single variable domains to adapt a proper structure that allows them to interact specifically with target molecules in the cytoplasm. Utilization of properly designed single domain intrabodies could circumvent technical problem associated with ordinary intrabodies, such as cleavage of the intradomain disulfide bonds or improper folding of the variable region, mainly due to highly reducing cytoplasmic conditions⁸.

The leader signal peptide promotes the secretion of the newly synthesized antibodies. However, localization of anti-WASP SHL, SV_H, and SV_L with their leader sequences was detected not only in the membrane fraction but also in the cytoplasmic fraction in T cells from each Tg mice (Fig. 1e). In addition, anti-WASP SHL, SV_H, and SV_L were not detected in the T-cell culture supernatant (data not shown). Immunoglobulin heavy and light chains are cotranslocated and assembled with disulfide bonds in the ER lumen. An ER resident chaperon, Bip, binds to the constant region of immunoglobulin and maintains the integrity of the immunoglobulin form during translocation from ER to the secretory pathway^{28,29}. Anti-WASP SHL, SV_H, and SV_L compose of only the variable regions, but not the constant regions of immunoglobulin, suggesting that the SHL, SV_H, and SV_L cannot be led to the inherent processing of the newly synthesized immunoglobulin.

Previously, we demonstrated that four types of anti-WASP single domains (SV_H, V_H, SV_L, and V_L) were expressed at similar levels regardless of the presence of the leader sequences in NIH3T3 cells²⁰. However, in both murine and human T cells, the expression levels of SV_H and SV_L constructs with the leader sequences were greatly higher than V_H and V_L constructs which lack the leader sequences, as similar to anti-WASP scFv constructs (Fig. 1, b and c). These results suggest that the expression pattern of scFv and single domain constructs with or without their leader sequences may be different among cell types. Furthermore, the expression efficiency of the

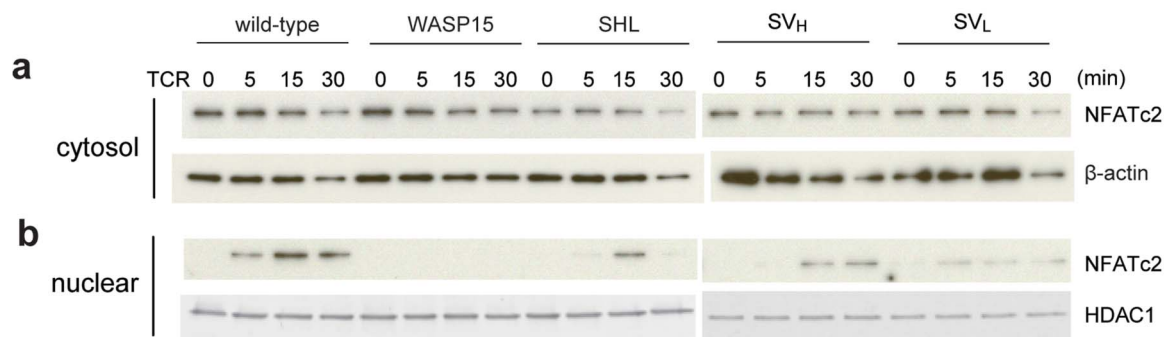


Figure 6 | Impaired nuclear translocation of NFAT after TCR stimulation in T cells from WASP15 Tg, anti-WASP SHL Tg, SV_H Tg, and SV_L Tg mice. TCR-stimulated T cell extracts from wild-type, WASP15 Tg, anti-WASP SHL Tg, SV_H Tg, and SV_L Tg mice were separated into (a) cytosolic and (b) nuclear protein fractions. The fractionated cell extracts were analyzed by Western blotting with anti-NFATc2 pAb, anti- β -actin pAb, or anti-HDAC1 pAb. Full-length gels/blots are presented in Supplemental Fig. 6. Immunoblots are representative of three independent experiments.



recombinant antibody fragments with or without signal sequences may depend on the character of parental monoclonal antibody clones.

T cells from anti-WASP SV_H/SV_L Tg mice exhibited impaired IL-2 production upon TCR stimulation, at levels similar to those observed in T cells from anti-WASP SHL Tg mice (Fig. 2). Furthermore, the proliferative response and IL-2 production induced by secondary OVA stimulation were impaired in lymphoid cells from anti-WASP SV_H/SV_L Tg mice immunized with OVA (Fig. 4, a and b). These results indicate that anti-WASP SV_H/SV_L single domains inhibit the function of N-terminal domain of WASP in the immune response in T cells as efficiently as their parental anti-WASP scFv. In contrast, actin polymerization and antigen receptor capping in anti-WASP SHL, SV_H, and SV_L Tg T cells induced by TCR stimulation were unaffected (Fig. S3 and S4). Previously, we demonstrated that dominant negative expression of WASP N-terminal domain (WASP15) also affected IL-2 production, but not affected TCR capping upon TCR stimulation¹⁸. Therefore, the WASP N-terminal domain has a critical role in IL-2 production, but not in actin cytoskeletal rearrangement after TCR signaling. Target-specific inhibition by anti-WASP N-terminal scFv, SV_H, and SV_L intrabodies strongly implicates the functional N-terminal domain of WASP in the T cell immune response. So, scFv and single domain intrabodies to WASP N-terminal domain would provide valuable tools to understand WASP downstream signaling pathways and function. Furthermore, the use of single domain intrabodies could be considered for potential therapeutic strategy against immunological disorders.

On the other hand, T lymphocytes from WAS patients with mutations in the N-terminal domain exhibit defects of both IL-2 production and cytoskeletal rearrangement upon TCR stimulation, which are similar to that of WASP knockout mice^{14–16}. In addition, expression of WASP was null or barely detectable level in T cells from these WAS patients¹⁷. In contrast, the expression level of WASP was comparable between wild-type and Tg mice T cells (Fig. 5e). As de la Fuente et al.²⁴ demonstrated, the binding of WIP and WASP is essential for the stability of WASP in T cells, however WIP-WASP interaction was strongly interfered by the anti-WASP intrabodies in Tg mice T cells (Fig. 5d). So, WASP may be somehow stabilized in our transgenic mice. The binding of anti-WASP intrabodies to the N-terminal domain of WASP might stabilize WASP as WIP does in wild-type mice, but this speculation needs to be verified.

Recently, we demonstrated that the WASP N-terminal domain specifically binds to the SH3 domain of Fyn tyrosine kinase in T cells. The interaction between WASP and Fyn was strongly inhibited by overexpression of the WASP N-terminal domain (WASP15) and anti-WASP scFv in T cells from each Tg mouse line²². In T cells from anti-WASP SV_H/SV_L single domain Tg mice, both SV_H and SV_L single domains were efficiently expressed and specifically bound to the WASP N-terminal domain (Fig. 1d), and inhibited specific interaction between WASP and Fyn by masking this domain (Fig. 5, a and c). Furthermore, TCR-induced tyrosine phosphorylation of WASP was diminished in T cells from anti-WASP SV_H/SV_L single domain Tg mice (Fig. 5f). These results strongly suggest that the phosphorylation of WASP upon TCR stimulation is induced by the association of activated Fyn with the WASP N-terminal domain in T cells.

In addition, T cells from WASP15 Tg, anti-WASP scFv Tg, SV_H Tg, and SV_L Tg mice exhibited impaired nuclear translocation of NFATc2 after TCR stimulation (Fig. 6). Badour et al.³⁰ demonstrated that TCR-induced phosphorylation of the WASP tyrosine residue at position 291 in human, and at position 293 in mouse, is required to induce NFAT translocation. Furthermore, by analyzing of a series of WASP deletion mutants, Silvin et al.³¹ demonstrated that the WASP homology 1 (WH1)/EVH1 domain, located in the WASP N-terminus, was responsible for NFAT transcriptional activity. Therefore, the specific interaction between Fyn and WASP through the

N-terminal domain is necessary for the nuclear translocation of activated NFAT in T cells. The identification of molecules downstream of the Fyn-WASP-WIP complex in the TCR signaling cascade will provide insight into the molecular mechanism underlying IL-2 production in T cells.

As shown in Fig. 2 and 3, the inhibitory effects differ among the intervention strategies exploited: dominant-negative WASP15 exhibited the strongest level of inhibition, while anti-WASP scFv, SV_H, and SV_L exhibited moderate inhibition of IL-2 synthesis and T cell proliferation upon TCR stimulation. Over-expressed WASP15 specifically binds to the Fyn SH3 domain and strongly inhibits the interaction between Fyn and endogenous WASP. In addition, the Fyn SH3 domain may interact not only with the WASP N-terminus, but also with other proline-rich regions (PRRs) containing signaling molecules that play important roles in TCR signaling. As a result, WASP15 overexpression may broadly interfere the function of Fyn during TCR signaling. Unlike the overexpression of WASP15, anti-WASP scFv, SV_H, and SV_L intrabodies specifically bind to the WASP N-terminal domain, and masking this domain does not affect the function of the Fyn SH3 domain. Therefore, the difference in the magnitude of inhibition of IL-2 production may be explained by the difference in action mechanisms of the two interventions between WASP15 and anti-WASP N-terminus intrabodies.

Intrabody technology can be used both to elucidate disease mechanisms and to provide novel therapies. Particularly, in the pharmaceutical area, intrabodies have the potential to be a powerful tool for target discovery and validation. Intrabodies offer the possibility of selectively blocking the functions of a target molecule on a domain-specific or epitope-specific basis. Because each single domain intrabody contains only one variable region against the target epitope, the structural analysis of the docking site of the single domain may predict small compounds, which may have biological activity and specificity similar to that of the single domain³². Alternatively, the single domain intrabody itself would work as a therapeutic device after the transfection of intrabody DNA or protein. Regarding the latter case, recent technologies to deliver antibody or enzyme to the inside of target cells have been reported, such as peptide-mediated delivery using protein-transducing peptides (PTDs)^{33,34}, or protein transfection using polyethyleneimine (PEI) as a transmembrane carrier³⁵. Furthermore, the delivery of antibody-conjugated nanoparticles to the cytoplasm interrupted specific cell signaling^{36,37}. Because of its minute size, the single domain fragment itself could easily be delivered into the cytoplasm, and might also be suitable for combining other application tools for target cell delivery. Finally, screening for or designing small-molecule drugs with the biological features of these anti-WASP single domain intrabodies may provide us with new, beneficial immunosuppressive agents.

Methods

Cells and electroporation. Expression vectors pCAG/SHL, HL, SV_H, V_H, SV_L, or V_L containing Myc-tagged anti-WASP scFv, V_H, or V_L constructs with or without the native leader signal sequences have been described previously^{19,20}. The murine T-cell hybridoma DO-11.10³⁸ and Jurkat cell line were maintained in RPMI 1640 medium supplemented with 100 U/ml penicillin, 100 µg/ml streptomycin, 4 mM L-glutamine, 50 µM 2-mercaptoethanol (2-ME), 10 mM Hepes (all obtained from Life Technologies, Carlsbad, CA, USA), and 10% fetal calf serum (FCS). DO-11.10 cells and Jurkat cells, adjusted to a concentration of 5 × 10⁶ cells/400 µl culture medium with 1.25% dimethyl sulfoxide per cuvette, were electroporated using a Gene Pulser (Bio-Rad, Hercules, CA, USA) with 40 µg plasmid DNA at 290V and 960 µF.

Generation of transgenic mice. The transgenes were excised from these expression vectors with *Sall*/*NheI* restriction enzymes, purified using agarose gel electrophoresis and a QIAquick Gel Extraction kit (Qiagen, Hilden, Germany), adjusted to a final concentration of 3 µg/ml, and microinjected into the fertilized egg pronuclei of inbred C57BL/6 mice. Next the injected eggs were then transferred into the oviducts of pseudopregnant female ICR mice. WASP15 Tg mice and anti-WASP SHL Tg mice were described previously^{18,19}. Procedures involving animal subjects have been approved by the Institutional Animal Care and Use Committee at the National Institute of Agrobiological Sciences (approval ID: H19-001-1).



Preparation of T cells. T cells were isolated from the spleens of WASP15 Tg, anti-WASP SHL Tg, SV_H Tg, SV_L Tg mice, and age-matched C57BL/6 mice, and purified by negative selection using microbeads conjugated to mouse CD45R (B220) antibodies (Miltenyi Biotec, Bergisch Gladbach, Germany) using the autoMACSTM system (Miltenyi Biotec) according to the manufacturer's instructions. The purity of the resulting T-cell population was >80% by fluorescence-activated cell sorting analysis with FITC-conjugated anti-mouse CD3 antibody (BioLegend, San Diego, CA, USA).

Quantitative real-time PCR. Purified T cells (1×10^7 cells) were seeded in 100-mm plastic dishes pre-coated with anti-CD3 ϵ antibody (145-2C11, BioLegend) at 20 μ g/ml and cultured at 37°C in RPMI 1640 medium containing 10% fetal calf serum (FCS) for 14 h. RNA from the stimulated T cells was isolated using the SV total RNA isolation system (Promega, Madison, WI, USA). cDNA was obtained using the ReverTra Ace- α TM first strand cDNA synthesis kit (Toyobo, Osaka Japan) according to the manufacturer's instructions, and amplified with the LightCycler TaqMan Master kit (Roche Diagnostics, Mannheim, Germany).

Real-time PCR for mouse IL-2 was performed in a LightCycler 1.5 (Roche) using Universal ProbeLibrary probe #15 (Roche) and IL-2 primers (forward, 5'-GCTG TTGATGGACCTACAGGA-3'; reverse, 5'-ATCCTGGGGAGTTTCAGGTT-3'). Mouse hypoxanthine phosphoribosyltransferase (HPRT) was employed as a relative standard, using Universal ProbeLibrary probe #22 (Roche) and HPRT primers (forward, 5'-TGATAGATCCATTCCTATGACTGTAGA-3'; reverse, 5'-AAGACA TTCTTCCAGTTAAAGTTGAG-3').

IL-2 ELISA. Purified T cells (1×10^6 cells) were seeded in 48-well tissue culture plates pre-coated with anti-CD3 ϵ antibody and cultured at 37°C in RPMI 1640 medium containing 10% FCS for 24 h. The IL-2 levels in culture supernatants were quantified in triplicate with the ELISA MAXTM Set Deluxe (BioLegend) according to the manufacturer's instructions.

T cell proliferation assay. Purified T cells (5×10^4 cells) were seeded in 96-well tissue culture plates pre-coated with anti-CD3 ϵ antibody and cultured at 37°C in RPMI 1640 medium supplemented with 100 U/ml penicillin, 100 μ g/ml streptomycin, 4 mM L-glutamine, 50 μ M 2-mercaptoethanol (2-ME), 10 mM Hepes, and 10% FCS with or without added IL-2 (5 ng/ml; Roche Diagnostics). After incubation for 48 h, 10 μ M 5-bromo-2'-deoxyuridine (BrdU) was added to the T cell cultures. The cells were incubated for an additional 16 h, and then BrdU incorporation during DNA synthesis in proliferating cells was quantified in triplicate with the Cell Proliferation ELISA (Roche Diagnostics) according to the manufacturer's instructions.

Immunization. Wild-type, WASP15 Tg, anti-WASP SHL Tg, SV_H Tg, and SV_L Tg mice were immunized in both footpads with 100 μ g of OVA (Sigma-Aldrich, St Louis, MO, USA) in TiterMax Gold (water-in oil adjuvant) (TiterMax, Norcross, GA, USA) on day 0. On day 7, inguinal, popliteal, and periaortic lymph nodes were removed, and then cells were suspended in RPMI 1640 medium containing 1% normal mouse serum. To examine proliferation, 1×10^5 cells were seeded in each well of 96-well tissue culture plates and cultured with the indicated amount of OVA or control BSA at 37°C for 48 h, then 10 μ M BrdU was added to the lymphoid cell cultures. The cells were incubated for an additional 16 h, and then BrdU incorporation during DNA synthesis in proliferating cells was quantified in triplicate with the Cell Proliferation ELISA (Roche Diagnostics). The maximal stimulation index was calculated as absorbance (A_{450} – A_{690}) of BrdU incorporation in OVA or control BSA-treated cells/absorbance of BrdU incorporation in untreated cells.

To evaluate IL-2 production induced by OVA stimulation, lymphoid cells (1×10^6 cells) were cultured with the indicated amount of OVA in 48-well tissue culture plates for 24 h. The IL-2 levels in culture supernatants were quantified in triplicate with the ELISA MAXTM Set Deluxe (BioLegend) according to the manufacturer's instructions.

Immunoprecipitation and Western blot analysis. The gene-transfected DO-11.10 cells, Jurkat cells, and purified T cells (1×10^8 cells) were lysed with RIPA buffer (50 mM Tris-HCl, pH7.6, 150 mM NaCl, 1% Nonidet P-40, 0.5% sodium deoxycholate and containing protease inhibitor cocktail) (Nacalai Tesque, Kyoto, Japan) on ice for 1 h. Cell lysates were centrifuged at 10 000 g for 10 min at 4°C, and the supernatants were incubated with 100 μ l of protein G-sepharose (GE Healthcare, Buckinghamshire, England) for 1 h at 4°C to remove nonspecifically bound proteins. The cleared lysates were incubated with 5 μ g of anti-Myc-tag mAb (MBL, Nagoya, Japan), anti-Fyn mAb, or anti-WIP pAb (Santa Cruz Biotechnology, Santa Cruz, CA, USA) on ice overnight, and then immunoprecipitated with 50 μ l of protein G-sepharose. Purified T cells stimulated by anti-CD3 ϵ antibody were lysed and incubated with 50 μ l of agarose-conjugated anti-phosphotyrosine (p-Tyr) mAb (Santa Cruz Biotechnology) at 4°C overnight. After washing five times with PBS, the immunocomplexes were resuspended in SDS sample buffer and boiled for 10 min.

Cell lysates and immunocomplexes were separated by SDS-PAGE (12.5 or 15% gel) and transferred to a polyvinylidene difluoride membrane (Bio-Rad, Hercules, CA, USA). The membrane was blocked with Blocking One (Nacalai Tesque) for 1 h at room temperature and probed with anti-WASP polyclonal antibody (pAb) raised against a synthetic peptide representing WASP residues (224–238) (Upstate, Lake Placid, NY, USA), anti-Fyn pAb, anti-WIP pAb, anti- β -actin mAb, anti-Ribophorin I pAb (Santa Cruz Biotechnology), anti-T7 pAb and anti-Myc pAb (MBL), and anti-nuclear factor of activated T cells (NFAT) c2 pAb or anti-histone deacetylase 1 (HDAC1) pAb (Santa Cruz Biotechnology), followed by horseradish peroxidase

(HRP)-conjugated anti-rabbit, anti-mouse, or anti-goat immunoglobulins (Dako, Glostrup, Denmark). Immunoreactive proteins were detected using Chemi-Lumi One L (Nacalai Tesque).

GST pull-down assay. Purified T cells (2×10^7 cells) were lysed with RIPA buffer on ice for 1 h. The lysates were centrifuged at 10 000 g for 10 min at 4°C, and the supernatants were incubated with 100 μ l of glutathione sepharose beads (GE Healthcare) for 1 h at 4°C to remove nonspecifically binding proteins. The cleared cell lysates were incubated with glutathione sepharose beads bound to 50 μ g of GST fusion protein at 4°C overnight. Beads were washed with PBS, lysed with SDS sample buffer, and immunoblotted with anti-WASP pAb and anti-GST pAb (Santa Cruz Biotechnology). The GST-Fyn-SH3 fusion protein has been described elsewhere³⁹.

Subcellular protein extraction. Cell extracts from wild-type, WASP15 Tg, anti-WASP SHL Tg, SV_H Tg, and SV_L Tg T cells were fractionated by the ProteoExtractTM Subcellular Proteome Extraction Kit (Calbiochem, San Diego, CA, USA) according to the manufacturer's instructions.

Statistical analysis. Statistical significance was assessed using Student's *t*-test (Statistica 03j; Tulsa, OK, USA). Differences were considered statistically significant when *P*-values were <0.05.

- Bird, R. E. *et al.* Single-chain antigen-binding proteins. *Science* **242**, 423–426 (1988).
- Huston, J. S. *et al.* Protein engineering of antibody binding sites: recovery of specific activity in an anti-digoxin single-chain Fv analogue produced in *Escherichia coli*. *Proc Natl Acad Sci USA* **85**, 5879–5883 (1988).
- Marasco, W. A., Haseltine, W. A. & Chen, S. Y. Design, intracellular expression, and activity of a human anti-human immunodeficiency virus type 1 gp120 single-chain antibody. *Proc Natl Acad Sci USA* **90**, 7889–7893 (1993).
- Steinberger, P., Andris-Widhopf, J., Buhler, B., Torbett, B. E. & Barbas, C. F. III Functional deletion of the CCR5 receptor by intracellular immunization produces cells that are refractory to CCR5-dependent HIV-1 infection and cell fusion. *Proc Natl Acad Sci USA* **97**, 805–810 (2000).
- Alvarez, R. D. *et al.* A cancer gene therapy approach utilizing an anti-erbB-2 single-chain antibody-encoding adenovirus (AD21): a phase I trial. *Clin Cancer Res* **6**, 3081–3087 (2000).
- Tanaka, T. & Rabbitts, T. H. Intrabodies based on intracellular capture frameworks that bind the RAS protein with high affinity and impair oncogenic transformation. *EMBO J* **22**, 1025–1035 (2003).
- Caron de Fromental, C. *et al.* Restoration of transcriptional activity of p53 mutants in human tumour cells by intracellular expression of anti-p53 single chain Fv fragments. *Oncogene* **18**, 551–557 (1999).
- Cattaneo, A. & Biocca, S. The selection of intracellular antibodies. *Trends Biotechnol* **17**, 115–121 (1999).
- Lobato, M. N. & Rabbitts, T. H. Intracellular antibodies and challenges facing their use as therapeutic agents. *Trends Mol Med* **9**, 390–396 (2003).
- Hamers-Casterman, C. *et al.* Naturally occurring antibodies devoid of light chains. *Nature* **363**, 446–448 (1993).
- Holt, L. J., Herring, C., Jespers, L. S., Woolven, B. P. & Tomlinson, I. M. Domain antibodies: proteins for therapy. *Trends Biotechnol* **21**, 484–490 (2003).
- Ochs, H. D. *et al.* The Wiskott–Aldrich syndrome: studies of lymphocytes, granulocytes, and platelets. *Blood* **55**, 243–252 (1980).
- Remold-O'Donnell, E., Rosen, F. S. & Kenney, D. M. Defects in Wiskott–Aldrich syndrome blood cells. *Blood* **87**, 2621–2631 (1996).
- Snapper, S. B. *et al.* Wiskott–Aldrich syndrome protein-deficient mice reveal a role for WASP in T but not B cell activation. *Immunity* **9**, 81–91 (1998).
- Zhang, J. *et al.* Antigen receptor-induced activation and cytoskeletal rearrangement are impaired in Wiskott–Aldrich syndrome protein-deficient lymphocytes. *J Exp Med* **190**, 1329–1342 (1999).
- Molina, I. J., Sancho, J., Terhorst, C., Rosen, F. S. & Remold-O'Donnell, E. T cells of patients with the Wiskott–Aldrich syndrome have a restricted defect in proliferative responses. *J Immunol* **151**, 4383–4390 (1993).
- Zhu, Q. *et al.* Wiskott–Aldrich syndrome/X-linked thrombocytopenia: WASP gene mutations, protein expression, and phenotype. *Blood* **90**, 2680–2689 (1997).
- Sato, M. *et al.* Overexpression of the Wiskott–Aldrich syndrome protein N-terminal domain in transgenic mice inhibits T cell proliferative responses via TCR signaling without affecting cytoskeletal rearrangements. *J Immunol* **167**, 4701–4709 (2001).
- Sato, M. *et al.* Intrabodies against the EVH1 domain of Wiskott–Aldrich syndrome protein inhibit T cell receptor signaling in transgenic mice T cells. *FEBS J* **272**, 6131–6144 (2005).
- Sawahata, R., Sato, M. & Kitani, H. Cytoplasmic expression and specific binding of the V_H/V_L single domain intrabodies in transfected NIH3T3 cells. *Exp Mol Pathol* **86**, 51–56 (2009).
- Miki, H., Miura, K. & Takenawa, T. N-WASP, a novel actin-polymerizing protein, regulates the cortical cytoskeletal rearrangement in PIP2-dependent manner downstream of tyrosine kinases. *EMBO J* **15**, 5326–5335 (1996).
- Sato, M., Sawahata, R., Takenouchi, T. & Kitani, H. Identification of Fyn as the binding partner for the WASP N-terminal domain in T cells. *Int Immunol* **23**, 493–502 (2011).



23. Ramesh, N., Anton, I. M., Hartwig, J. H. & Geha, R. S. WIP, a protein associated with Wiskott–Aldrich syndrome protein, induces actin polymerization and redistribution in lymphoid cells. *Proc Natl Acad Sci USA* **94**, 14671–14676 (1997).
24. de la Fuente, M. A. *et al.* WIP is a chaperone for Wiskott–Aldrich syndrome protein (WASP). *Proc Natl Acad Sci USA* **104**, 926–931 (2007).
25. Jain, J., Loh, C. & Rao, A. Transcriptional regulation of the IL-2 gene. *Curr Opin Immunol* **7**, 333–342 (1995).
26. Rao, A., Luo, C. & Hogan, P. G. Transcriptional factors of the NFAT family: regulation and function. *Annu Rev Immunol* **15**, 707–747 (1997).
27. Tanaka, T. & Rabbits, T. H. Functional intracellular antibody fragments do not require invariant intra-domain disulfide bonds. *J Mol Biol* **376**, 749–757 (2008).
28. Munro, S. & Pelham, H. R. An Hsp70-like protein in the ER: identity with the 78 kd glucose-regulated protein and immunoglobulin heavy chain binding protein. *Cell* **46**, 291–300 (1986).
29. Flynn, G. C., Pohl, J., Flocco, M. T. & Rothman, J. E. Peptide-binding specificity of the molecular chaperone Bip. *Nature* **353**, 726–730 (1991).
30. Badour, K. *et al.* Fyn and PTP–PEST-mediated regulation of Wiskott–Aldrich syndrome protein (WASP) tyrosine phosphorylation is required for coupling T cell antigen receptor engagement to WASp effector function and T cell activation. *J Exp Med* **199**, 99–112 (2004).
31. Silvin, C., Belisle, B. & Abo, A. A role for Wiskott–Aldrich syndrome protein in T-cell receptor-mediated transcriptional activation independent of actin polymerization. *J Biol Chem* **276**, 21450–21457 (2001).
32. Stocks, M. Intrabodies as drug discovery tools and therapeutics. *Curr Opin Chem Biol* **9**, 359–365 (2005).
33. Heng, B. C. & Cao, T. Making cell-permeable antibodies (Transbody) through fusion of protein transduction domain (PTD) with single chain variable fragment (scFv) antibodies: potential advantages over antibodies expressed within the intracellular environment (Intrabody). *Med Hypotheses* **64**, 1105–1108 (2005).
34. Zhao, Y., Lou, D., Burkett, J. & Kohler, H. Chemical engineering of cell penetrating antibodies. *J Immunol Methods* **254**, 137–145 (2001).
35. Didenko, V. V., Ngo, H. & Baskin, D. S. Polyethyleneimine as a transmembrane carrier of fluorescently labeled proteins and antibodies. *Anal Biochem* **344**, 168–173 (2005).
36. Bale, S. S. *et al.* Nanoparticle-mediated cytoplasmic delivery of proteins to target cellular machinery. *ACS NANO* **4**, 1493–1500 (2010).
37. Shah, D. A. *et al.* Regulation of stem cell signaling by nanoparticle-mediated intracellular protein delivery. *Biomaterials* **32**, 3210–3219 (2011).
38. Simonkevitz, R., Kappler, J., Marrack, P. & Grey, H. Antigen recognition by H-2-restricted T cells. I. Cell-free antigen processing. *J Exp Med* **158**, 303–316 (1983).
39. Takemoto, Y., Sato, M., Furuta, M. & Hashimoto, Y. Distinct binding pattern of HS1 to the Src SH2 and SH3 domains reflect possible mechanisms of recruitment and activation of downstream molecules. *Int Immunol* **8**, 1699–1705 (1996).

Acknowledgments

This work was supported in part by the NIAS Strategic Research Fund and the Animal Genome project of the Ministry of Agriculture, Forestry and Fisheries of Japan.

Author contributions

M.S. and H.K. conceived and designed the experiments. M.S. and R.S. performed the experiments. C.S. and T.T. assisted with experiments and commented on the manuscript. M.S. and H.K. wrote the manuscript.

Additional information

Supplementary information accompanies this paper at <http://www.nature.com/scientificreports>

Competing financial interests: The authors declare no competing financial interests.

How to cite this article: Sato, M., Sawahata, R., Sakuma, C., Takenouchi, T. & Kitani, H. Single domain intrabodies against WASP inhibit TCR-induced immune responses in transgenic mice T cells. *Sci. Rep.* **3**, 3003; DOI:10.1038/srep03003 (2013).



This work is licensed under a Creative Commons Attribution-NonCommercial-ShareAlike 3.0 Unported license. To view a copy of this license, visit <http://creativecommons.org/licenses/by-nc-sa/3.0>